



# Effect of Nano CuO Doping on Structural, Thermal and Optical Properties of PVA/PEG Blend

Ali A. Alhazime<sup>1</sup>

Received: 17 March 2020 / Accepted: 4 May 2020 / Published online: 18 May 2020  
© Springer Science+Business Media, LLC, part of Springer Nature 2020

## Abstract

Copper oxide (CuO) nanoparticles were synthesized by sol gel method. Copper oxide/polyvinyl alcohol/polyethylene glycol (CuO/PVA/PEG) doped blends with concentrations (3%, 5%) of CuO nanoparticles were prepared by casting technique. X-ray diffraction data (XRD) and Fourier transform infrared (FTIR) techniques confirmed the formation of new-doped nano-blends. The absorption spectra revealed an apparent change with doping concentration. Different optical parameters were discussed in detail and proved to be directly affected by nanoparticles doping concentrations. The energy gap values for polymer blends decreased from 5.3 to 4.7 eV with the addition of CuO nanoparticles. The study of the effect of CuO nanoparticles incorporation in (PVA/PEG) blends has attracted a little interest in the literature; therefore, this study is considered as a new research one.

**Keywords** Nano CuO · PVA/PEG · XRD · Optical · Thermal

## 1 Introduction

Polyvinyl alcohol (PVA) is the most well-known versatile water soluble polymer characterized with a wide range of feasible applications in different industrial and research fields because of its magnificent characteristics such as biodegradable, biocompatible and highly adhesive material, excellent mechanical properties [1], low cost, ease of treatment as film forming, highly elastic and highly stable photosensitive material [2], high dielectric properties and good charge storage material [3]. PVA can be blended with other polymers to form polymer complexes by hydrogen bonding. Hydroxyl groups that is located on the carbon chain backbone of the polymer are considered the main source of the hydrogen bonding [4, 5]. On the other hand, polyethylene glycol (PEG) is a highly water soluble and nontoxic material, besides, its solubility in most organic solvents is considerably high. Moreover, when PEG mixed with other polymeric material, most of these properties can be shared within the resulting blend [6]. Introducing metal oxide nanoparticles into polymers varies the physical and chemical properties

of the resulting nanocomposite material. Of course, these properties depend on the type of the nanoparticles used and their preparation method. Many authors have investigated the effect of dispersing metal oxide nanoparticles into (PVA-PEG) polymer matrix and they represented detailed information about the compositional variations occurred. Titanium dioxide nanoparticles (TiO<sub>2</sub>) effect on (PVA-PEG) blends has been extensively studied and studies showed an enhancement in the humidity sensing behavior of (PVA-PEG) polymer blends [7] and an increase in their dielectricity and bioactivity behaviour and the samples were non-toxic [8–11]. Others observed an increment in the ionic conductivity of the (PVA-PEG) blends with the addition of TiO<sub>2</sub> nanoparticles [10].

Tin oxide (SnO<sub>2</sub>) elsewhere [12], improved the semiconducting behaviour and the optical conductivity of PVA-PEG blends. Magnesium oxide (MgO) nanoparticles in various weight percentages improved the optical properties of (PVA-PEG-MgO) nanocomposites [13]. Different concentrations (0.0, 0.5, and 1.0 wt%) of hematite ( $\alpha$ -Fe<sub>2</sub>O<sub>3</sub>) nanorods increased the optical attitude and the AC conductivity of (PVA-PEG) blends which is promising to future usage in a variety of optical and dielectric components in devices [14]. The zinc oxide nanoparticles ZnO proved its ability for boosting the optical properties of (PVA-PEG-ZnO) nanocomposites as well [15]. Boron Oxide (B<sub>2</sub>O<sub>3</sub>) enhanced the

✉ Ali A. Alhazime  
aborose1@hotmail.com

<sup>1</sup> Physics Department, Taibah University, Medinah, Munawara, Saudi Arabia

structural properties of PVA/PEG/ B<sub>2</sub>O<sub>3</sub> hybrid materials [9]. Copper oxide (CuO) as a transition-metal oxide is a covalent semiconductor material having relatively small band gap (from 1.21 to 1.5 eV). Among most common metal oxide nanoparticles, CuO ones which are of special prominence due to their ease of manufacture, low cost, nontoxic behaviour and high ability of optical absorption. It is also characterized by its crystalline structure, photoconductive, anti-ferromagnetic and thermodynamic properties besides instability attitude during chemical reactions [16–21]. CuO nanoparticles have been added to different polymeric materials to cover multiple technical purposes in many fields. Others showed that the optical parameters and the electrical conduction behaviour of PVA/CMC blends could be controlled and improved with the addition of CuO nanoparticles [22, 23]. Rabia et al. [24] investigated the effect of CuO nanoparticles on both PEG (polyethyleneglycol) and PVP (polyvinylpyrrolidone) and they proved validity of new nano-compounds to be used as antitumor materials. Others discussed the influence of CuO nanoparticles on the structural, thermal, mechanical and electrical properties of PVA [25–27] and investigated the antimicrobial activity of polypropylene [28–30]. No one in the literature up to now discussed the effect of adding CuO nanoparticles on the structural, optical and thermal characteristics of (PVA-PEG) blends which makes our research work as a brand new study. In this work a new nanocomposite blend materials (PVA-PEG/CuO) have been synthesized based on PVA, PEG and CuO nanoparticles by casting technique. Structural, optical and thermal studies were performed using (XRD) X-ray diffraction and (FTIR) Fourier transform infrared techniques, UV–Vis. Spectrophotometry technique and (TGA) Thermogravimetric analysis technique, respectively.

## 2 Experimental

Nano CuO was prepared by the sol gel method in which 0.5 g of copper nitrate (99.9%; Sigma-Aldrich Chemie GmbH, Munich, Germany), 10 g of citric acid (99.999%; Alfa Aesar GmbH & Co KG, A Johnson Matthey Company, Erlenbachweg 2, 76,870 Kandel, Germany) and 10 ml of ethylene glycol were mixed, heated at 90 °C and stirring in 10 ml of distilled water until the liquid is evaporated. The gel precursor then decomposed at 500 °C (1/2 h) in an electric oven [31].

PVA/PEG blend was prepared by casting method by dissolving 90% of polyvinyl alcohol (PVA) (degree of hydrolysis = 99%, molecular weight = 27,000 g/mol) and 10% Polyethylene glycol (PEG) (powder, molecular weight = 4000 g/mol) in distilled water under stirring at 80 °C until the solution became clear.

In case of CuO/PVA/PEG blends, the above similar mixture was then obeyed for ultrasonic at 60 °C for 2 h after addition of CuO nano particle in different ratio (3 and 5%) with respect to PVA/PEG blend according to the next formula:

$$x(\text{wt}\%) = \frac{w_f}{w_p + w_f} \times 100$$

where  $w_f$  and  $w_p$  are the weights of CuO and PVA/PEG blend, respectively.

The solution was casted into Petri dishes and placed for 3 days in a closed box, until the polymers films formed [31].

X-ray diffraction (Shimadzu 6000 X-ray diffractometer, CuK<sub>α</sub>) was used in order to insure the formation of nano CuO and investigate the homogeneity of CuO nano particle inside PVA/PEG blend. Morphology of the nano sample was identified using transmission electron microscope (TEM, JEOL JEM-100CX). Thermogravimetric analysis (TGA) was carried by Perkin Elmer TGA instrument with heating rate = 10 °C/min under ambient atmosphere air (35–500 °C). The different optical parameters for the different blends were determined by UV–Vis. Spectrophotometry (Model Tomos UV-1800) technique. Fourier transform infrared (FTIR) spectroscopy (Bruker Tensor 27 FTIR Spectrometer) was performed in the range of 500–3500 cm<sup>-1</sup> to verify the presence of nano CuO in PVA/PEG blends. Morphologies of PVA/PEG:CuO films were investigated by Jeol scanning electron microscope (SEM, JSM-6510A Model, Japan).

## 3 Results and Discussion

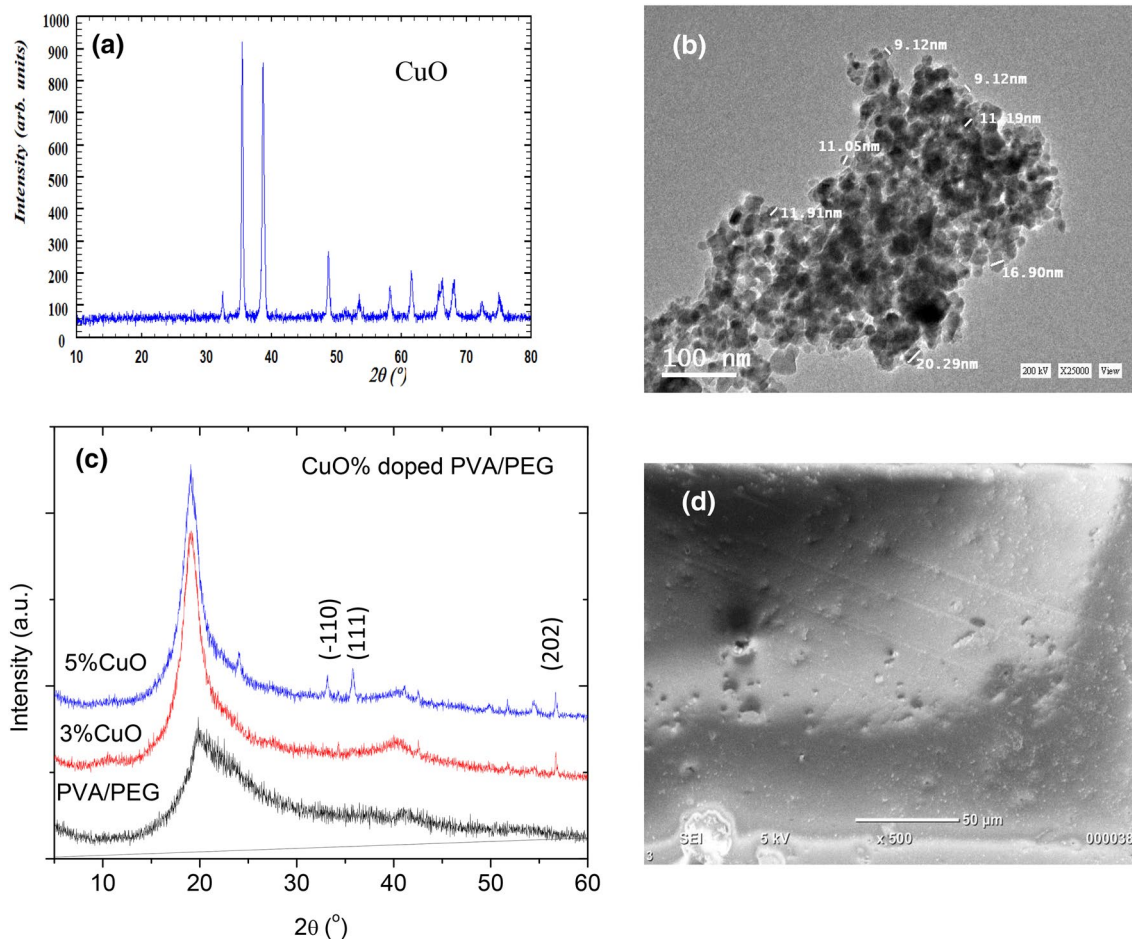
### 3.1 Structural Investigation

Figure 1a reveals the X-ray diffraction pattern from nano CuO. The diffraction pattern has a single phase with a monoclinic structure and lattice parameters  $a = 4.6871$ ,  $b = 3.4232$ , and  $c = 5.1323$  Å, which is good agreement with JCPDS card number 45–0937. The peak position at 32.36°, 35.33°, 38.56°, 48.53°, 58.10°, 61.436°, 66.18° and 68.05° are corresponding to the Miller indices (hkl) planes of the (–110), (111), (022), (–202), (202), (–113), (022) and (–220) planes of the monoclinic structure, respectively. The crystallite size of the sample was 15 nm which determined using Scherrer formula:

$$L = \frac{0.9\lambda}{\beta \cos\theta}$$

where  $\lambda$  and  $\beta$  are the wavelength and half of maximal intensity, respectively.

TEM micrograph of CuO nanoparticles is shown in Fig. 1b; nanoparticles were fine characterized with average



**Fig. 1** XRD diffractions for **a** nano CuO, **b** TEM image for CuO, **c** CuO doped PVA/PEG blends and **d** SEM image for 3% CuO doped PVA/PEG blends

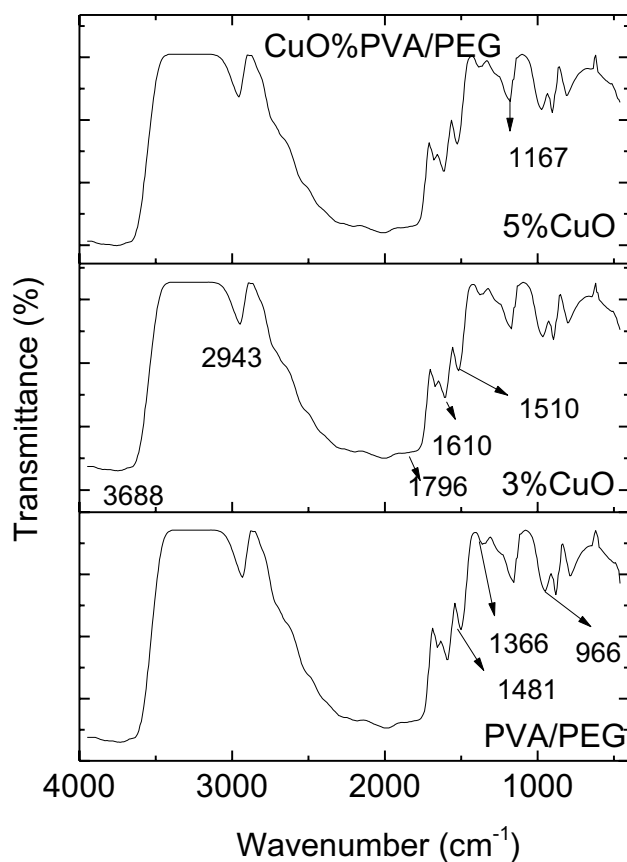
size about 20 nm which is a bit larger than the result got from XRD data. Figure 1c reveals the diffraction patterns of (PVA/PEG) and (CuO/PVA/PEG) blends samples were almost identical with the chief diffraction peak observed at  $2\theta=21^\circ$ , associated with the partial crystallinity of the structure [31]. Some diffraction peaks associated to CuO nanoparticles are indexed in the Fig. 1a, which confirmed the presence of CuO in PVA/PEG matrix. Figure 1d reveals SEM picture for (CuO/PVA/PEG) nano-blend. As seen, nano-CuO is well dispersed throughout the blend.

Figure 2 reveals the FTIR spectra in the wavenumber range of  $3500$  to  $500\text{ cm}^{-1}$  for the undoped and doped PVA/PEG blend with different concentrations of CuO (3% and 5%). The FTIR spectra for all samples revealed a broad band at  $3688\text{ cm}^{-1}$  corresponding to the stretching vibration  $\text{OH}^-$  groups [32], with a small shift in peak position that can be ascribed to the H-bond formation [33]. In addition, the band at  $2943\text{ cm}^{-1}$  attributed to the stretching  $\text{CH}_2$  group [34]. The band at around  $1610\text{ cm}^{-1}$  is demonstrating the deformation of vinyl alcohol [35]. The existence of

stretching  $\text{C}=\text{O}$  carbonyl group of the acetate group was established from the bands at  $1796$  and  $1510\text{ cm}^{-1}$  [36]. The bands around  $1481$ ,  $1366$  and  $1167\text{ cm}^{-1}$  associated with symmetry  $\text{CH}_2$  bond, stretching vibrations related to mixed  $\text{CH}^-$  and  $\text{OH}^-$  bending modes, and the  $\text{C}-\text{C}$  stretching mode associated with the regular repetition of the trans-configuration of the zigzag chain in a crystalline region, respectively [36]. The band at  $966\text{ cm}^{-1}$  is representing the syndiotactic structure with strong vibration [37]. Finally, the shifting in the bands positions pointed to the existence of CuO nanoparticles in the blend matrix.

### 3.2 Thermal Analysis

Figure 3 showed thermogravimetric analysis (TGA) of (PVA/PEG) and (CuO/PVA/PEG) nanocomposite polymers from room temperature to  $500^\circ\text{C}$  with a heating rate of  $10^\circ\text{C}/\text{min}$ . All nanocomposite polymer films revealed one degradation stage. This degradation stage had a peak at  $70^\circ\text{C}$  for (PVA/PEG) which increased to  $93^\circ\text{C}$  as amount of



**Fig. 2** IR for pure and CuO doped PVA/PEG blends

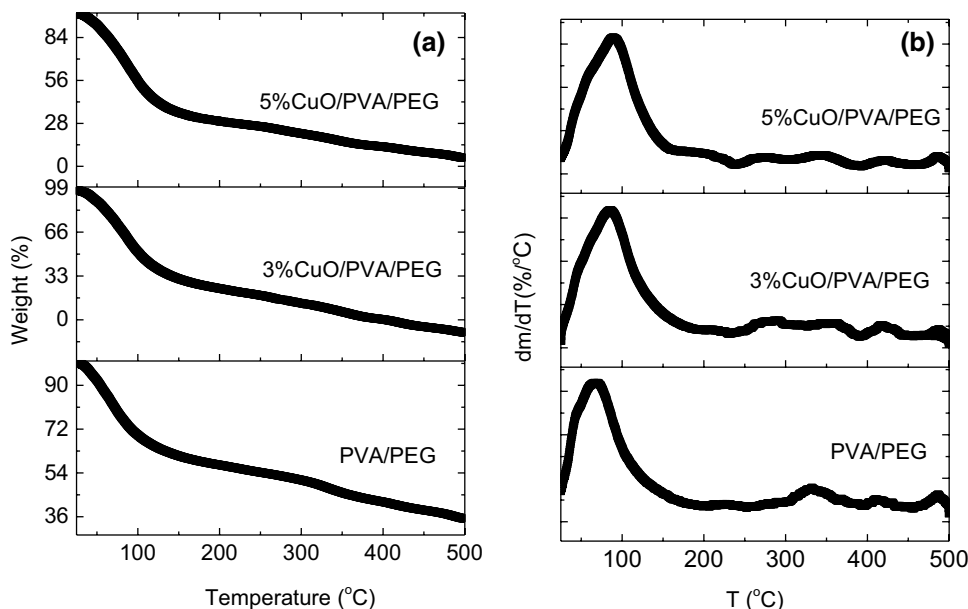
nano CuO doped PVA/PEG matrix became 5%. The weight loss was associated with the evaporation of the physically weak and chemically strong bound of H<sub>2</sub>O from the polymer

matrix [38]. From the figure, it is noticed that 5% CuO doped (PVA/PEG) blend has a highest thermal stability as compared with undoped and 3% CuO doped (PVA/PEG) blends. The improvement of the thermal stability upon doping of (PVA/PEG) with 5% CuO nanoparticles could be due to the interaction occurs between the nano CuO and the hydroxyl groups of the polymer blend [39]. Furthermore, the other fluctuations emerged in DTG at higher temperature, Fig. 3b, may be due to the degradation of the side chain (O–H) and the cleavage of C–C backbone (carbonation) of (PVA/PEG) polymer blend [40].

### 3.3 UV-Spectroscopy Analysis

The absorption figure for undoped PVA/PEG films and doped ones is shown in Fig. 4a. One can see an absorption rise with a faint peak centered at 300 nm in the UV region for both undoped and doped blends. These results are in similar agreement with those previously represented [41, 42]. No variation in the absorption peak position can be observed although different molecular weights of polymers used which agrees quite well with the literature [43]. The appearance of this absorption peak can be returned to the transitions of the unshared electron pairs upon unsaturated bonds C=C and C=O along the polymer structure. Similar investigations have been represented earlier [44]. An increase in these spectra can be observed with dopant concentration. These results are a clear proof for the occurrence of mutual interactions between nanoparticles and the polymer matrix. The increase in the absorption behavior with CuO nanoparticles can be returned to the formation of new intermolecular bonds between cations and anions forming defects along the whole polymer matrix [45]. A

**Fig. 3** Thermogravimetric curves for pure and CuO doped PVA/PEG blends



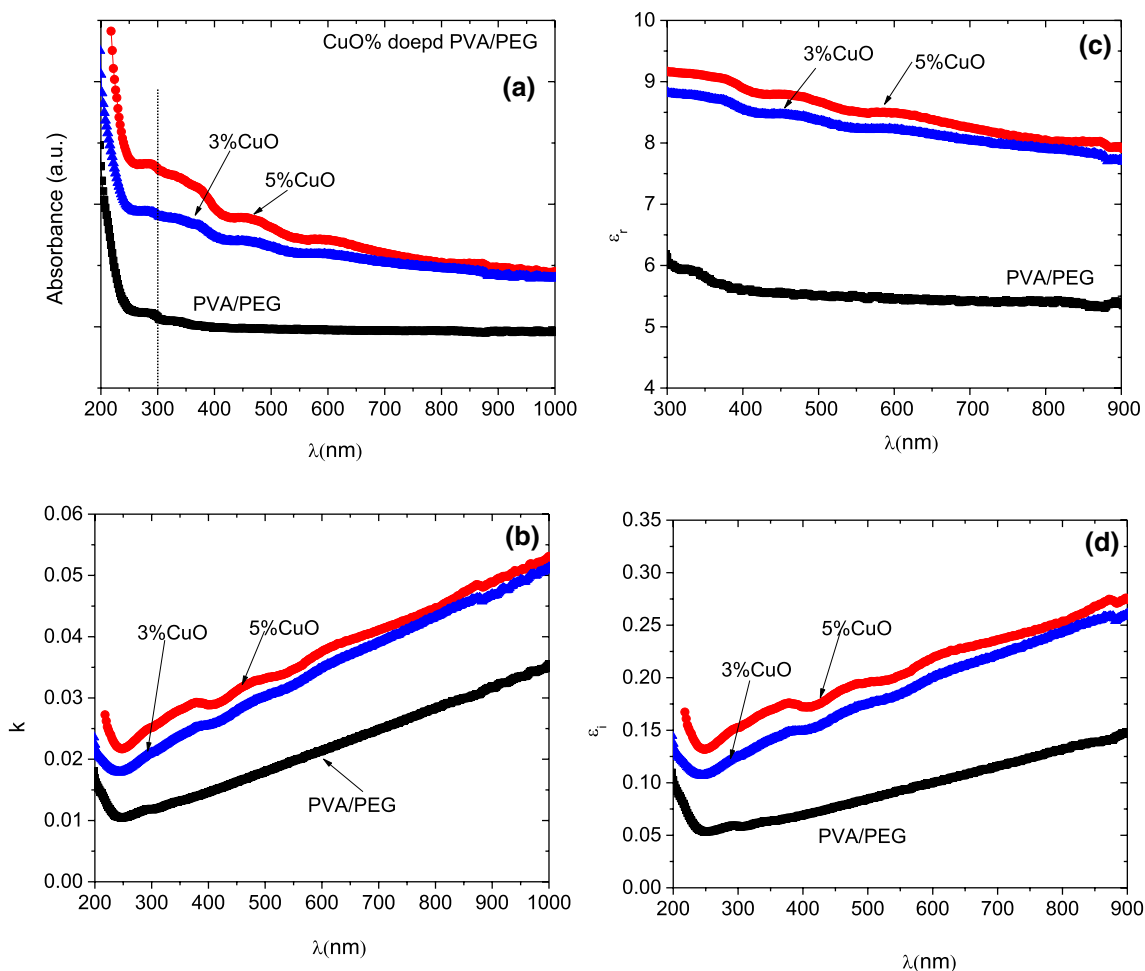


**Fig. 4** **a** UV–Vis absorbance, **b** extinction coefficient, **c** real part of dielectric constant and **d** dielectric loss for pure and CuO doped PVA/PEG blends

decrease in the absorption spectra within the optical range (300 to 800 nm) for all samples with the wavelength can be observed which is due to the decrease in the incident light energy [46, 47]. The increase in the absorption values with the nanoparticles content (3% and 5%) enhances the effect of doping. One can expect a gradual decrease in the transmittance values (figure not shown). This decrease in the transmittance values can be referred to the scattering process of the incident photons by denser nanoparticles. The counter behaviour between transmittance and absorption values with doping concentration shows the amorphous nature of PVA/PEG samples [48]. Optical constants such as the extinction coefficient ( $k$ ) and refractive index ( $n$ ) are necessary parameters for measuring the fraction of the dissipated energy per unit length of the material [49] and describing the polarizability behaviour of the molecules under the effect of the incident electromagnetic field [50], respectively. Both ( $k$ ) and ( $n$ ) are related to each other through the wellknown Lorentz–Lorentz relation [51, 52]

$$n = \frac{1+R}{1-R} + \sqrt{\frac{4R}{(1-R)^2} - k^2} \quad (1)$$

where  $k$  and  $\alpha$  are given as:

$$k = \frac{\lambda\alpha}{2\pi} \text{ and } \alpha(\lambda) = \left(\frac{2.303}{d}\right)A \quad (2)$$

where  $R$ ,  $\alpha$ ,  $\lambda$ ,  $A$  and  $d$  are the reflectance, the absorption coefficient, the wavelength, the absorbance and the sample thickness. The absorption coefficient  $\alpha$  is defined as the energy absorbed per unit length of the material in unit time [53]. Equation (2) confirms the similarity in behavior and peak position between extinction coefficient and the absorption spectra due to the direct relationship as shown in Fig. 4b. It is clear from the equation that as the amount of nanoparticles increases the fraction of light absorbed due to scattering increases as well [54]. Figure 5 shows the refractive index spectra for both undoped and doped samples. The

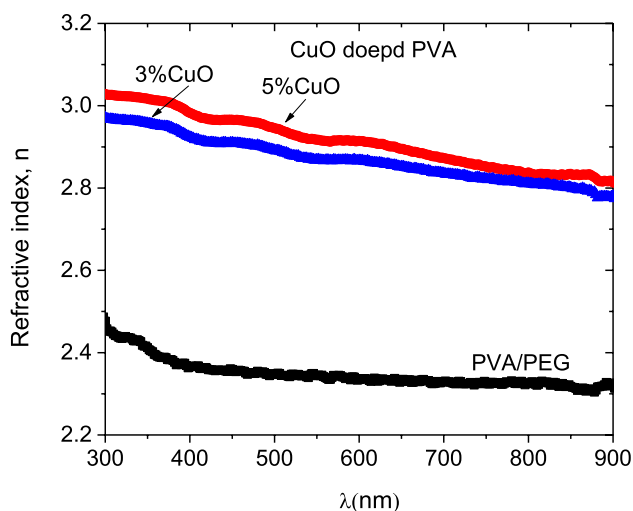


**Fig. 5** Wavelength dependent of refractive index for pure and CuO doped PVA/PEG blends

spectra exhibit faint dispersion peak in the low energy region for undoped PVA/PEG samples while this peak disappears in the case of doped ones. The spectra for all samples show a plateau shape in the low energy region. The refractive index spectra showed as increase with the content of nanoparticles doping which reflected the alignment occurred to the samples molecules due to the electromagnetic field of the incident light [55]. One can say that, increasing nanoparticles concentration affects the samples density (rises it) due to increasing the number of defects formed between added nanoparticles and OH groups, these defects are responsible for stressing the samples a rise in its density. No effect for the incident light on the samples molecules in the visible region which manifests the molecules inertia.

The real ( $\epsilon_r = n^2 - k^2$ ) and imaginary ( $\epsilon_i = 2nk$ ) parts of optical dielectric constant are important parameters because they are directly related to the energy density of states within the optical band gap of the material [56]. The dielectric function cannot be measured directly by an experimental procedure such as absorbance and transmittance [57]. It is clear that  $\epsilon_r$  and  $\epsilon_i$  are closely dependent on the values of refractive index  $n$  and extinction coefficient  $k$ .  $\epsilon_r$  describe the dispersion in the medium and  $\epsilon_i$  refers to the dissipated incident energy by the medium. The optical spectra of  $\epsilon_r$  and  $\epsilon_i$  for undoped and doped PVA/PEG samples are shown in Fig. 4c and d. It is clear from Fig. 4c that  $\epsilon_r$  exhibits a gradual decrease in the low energy region until it reaches a nearly constant attitude. This is not a surprising attitude which is similar to that of the refractive index and the extinction coefficient discussed before and confirms the role of the new defects formed between CuO nanoparticles and the polymer structure. Therefore, the rise in  $\epsilon_r$  values with nanoparticles concentrations can be returned to the structure modifications occurred because of the new

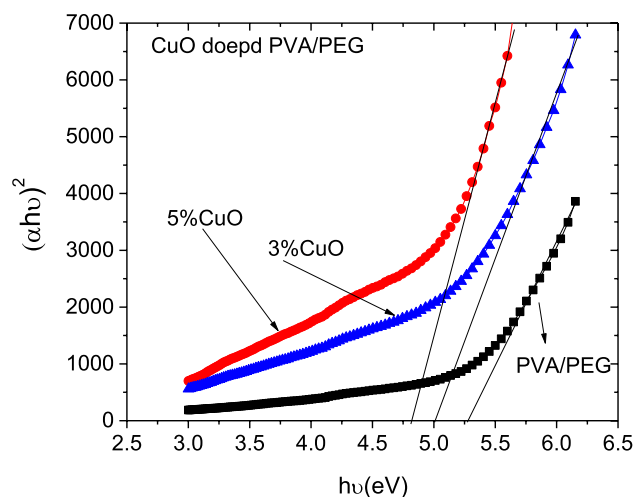


**Fig. 6** Energy dependence of  $(\alpha hv)^2$  for pure and CuO doped PVA/PEG blends

defects formed within the material increasing its density. Figure 4d represents the optical spectra of  $\epsilon_i$  for all undoped and doped samples. An increase in the  $\epsilon_i$  spectra with the wavelength can be observed besides a rise in the  $\epsilon_i$  spectral values with the nanoparticles concentration. This behaviour proofs the effect of both the refractive index and extinction coefficient. The behavior of  $\epsilon_i$  optical spectra is consistent with that of  $\epsilon_r$  for doping concentrations indicating that the highly doped PVA/PEG samples dissipate much more incident energy when compared to the films doped with lower concentrations.

The study of the absorption process in more details is very important for gathering information about the optical band gap structure and describing its possible electronic transitions. The band gap is defined as the energy gap between the valance and conduction bands. The direct optical energy gap  $E_g$  values can be calculated using the well-known famous Tauc equation [58, 59]:

$$\alpha hv = A(hv - E_g)^n \quad (3)$$

where  $h$ ,  $\nu$ ,  $A$  and  $n$  are Planck's constant, incident light frequency, is a constant and  $n$  is a parameter its values determines the type of transition; becomes 1/2 or 2 for direct allowed or indirect allowed band gap semiconductors, respectively [60–62]. Figure 6 represents the relation between  $(\alpha hv)^2$  (as y-axis) and  $(hv)$  as (x-axis) (direct allowed transition) for undoped and doped PVA/PEG samples. Referring to the figure, all samples show similar absorption edge behaviour and there is a shift towards the low energy region with increasing the nanoparticles doping concentration. The energy gap  $E_g$  values can be obtained by extrapolating the straight lines of the spectra to the point  $(\alpha hv)^2 = 0$  and taking the intersection values  $(hv)$  values). According to the graph,  $E_g$  values are found to be 5.3, 5 and

4.7 eV for undoped and doped (3% and 5%) respectively. Which means increasing the nanoparticles doping concentration from 3 to 5% decreases the  $E_g$  values from 5.3 eV (for undoped samples) to 5 and 4.7 eV respectively. These changes in the energy gap values can be interpreted as: the rise in the nano-dopant concentration increases the degree of disordering of the polymer material by introducing some defects (formed between CuO nanoparticles and OH groups) to the structure. These defects are responsible for the production of new localized states within band gap region, similar results to ours have been represented elsewhere [50, 63–65].

## 4 Conclusion

X-ray diffraction pattern (XRD) revealed that nano CuO has a monoclinic structure with crystallite size 15 nm. XRD confirmed also the dispersion of nano-CuO into PVA/PEG blend. FTIR of CuO/PVA/PEG blends exhibited a shift in the bands positions pointed to the existence of CuO nanoparticles in the blend matrix. Thermogravimetric analysis (TGA) demonstrated that 5% CuO doped (PVA/PEG) blend has a highest thermal stability, which could be due to the interaction, occurs between the nano CuO and the hydroxyl groups of the polymer blend. The blend absorbance was enhanced while its transmittance reduced as it doped with nano CuO. The absorbance and transmittance of the blend further increased and decreased as amount of CuO doping increased in the matrix, respectively. In addition, the dielectric constant and refractive index of the blend were improved as it doped with CuO, and their values increased as the amount of nano CuO doping increased in the blend. The energy gap decreased 5.3 eV for undoped blend to 5 and 4.7 eV for doped blends with 3% and 5% CuO, respectively, due to the creation of the disordering inside the blend matrix upon doping it with nano CuO.

## References

- W. Li, X. Zhao, Z. Huang, S. Liu, Nanocellulose fibrils isolated from BHKP using ultrasonication and their reinforcing properties in transparent poly (vinyl alcohol) films. *J. Polym. Res.* **20**(210), 1–7 (2013)
- K. Kannan, L. Guru Prasad, S. Agilan, N. Muthukumarasamy, Investigations on Ag<sub>2</sub>S/PVA-PEG polymer nanocomposites: an effectual nonlinear optical material. *Optik-Int. J. Light Electron Opt.* **170**, 10–16 (2018)
- A. Hassen, A.M. El Sayed, W.M. Morsi, S. El-Sayed, Influence of Cr<sub>2</sub>O<sub>3</sub> nanoparticles on the physical properties of polyvinyl alcohol. *J. Appl. Phys.* **112**(093525), 1–8 (2012)
- A.M. El Sayed, H.M. Diab, R. El-Mallawany, Controlling the dielectric and optical properties of PVA/PEG polymer blend via e-beam irradiation. *J. Polym. Res.* **20**(255), 1–10 (2013)
- I.R. Agool, K.J. Kadhim, A. Hashim, Preparation of (polyvinyl alcohol–polyethylene glycol–polyvinyl pyrrolidone–titanium oxide nanoparticles) nanocomposites: electrical properties for energy storage and release. *Int. J. Plast. Technol.* **20**, 121–127 (2016)
- T.R. Rao, K.V. Brahmam, C.L. Raju, Spectroscopic studies of Cr<sup>3+</sup> ions doped in poly(vinylalcohol) complexed polyethylene glycol polymer films. *AIP Conf. Proc.* **1661**, 110014 (2015)
- M. Joshi, R.P. Singh, Cross linking polymers (PVA & PEG) with TiO<sub>2</sub> nanoparticles for humidity sensing. *Sens. Transducers J.* **110**(11), 105–111 (2009)
- M. Diantoro, L.A. Sari, T. Istirohah, A.D. Kusumawati, Nasikhudin, Sunaryono, Control of dielectric constant and anti-bacterial activity of PVA-PEG/x-SnO<sub>2</sub> nanofiber. *IOP Conf. Ser: Mater. Sci. Eng.* **367**, 012012 (2018)
- H. Hristov, M. Nedyalkova, S. Madurga, V. Simeonov, Boron oxide glasses and nanocomposites: synthetic, structural and statistical approach. *J. Mater. Sci. Technol.* **33**(6), 535–540 (2017)
- H. Amiri, M. Mohsennia, Impedance study of PVA/PEG/LiClO<sub>4</sub>/TiO<sub>2</sub> nanocomposite solid polymer blend electrolyte. *J. Mater. Sci.: Mater. Electron.* **28**, 4586–4592 (2017)
- M. Diantoro, T. Istirohah, A. Fuad, I. Ristanti, Dielectric properties and bioactivity of PVA/PEG/TiO<sub>2</sub> fibers for capacitive based body sensor. *IOP Conf. Ser.: J. Phys.* **1040**, 012045 (2018)
- N.H. El Fewaty, A.M. El Sayed, R.S. Hafez, Synthesis, structural and optical properties of tin oxide nanoparticles and its CMC/PEG–PVA nanocomposite films. *Polym. Sci. Ser. A* **58**, 1004–1016 (2016)
- B.H. Rabee, N. Adel Hadi, Study the effect of nano-Mgo on the optical properties of (PVA-PEG-Mgo) Nanocomposites. *Int. J. Eng. Res. Technol.* **3**(6), 2257–2260 (2014)
- A.M. El Sayed, W.M. Morsi, a-Fe<sub>2</sub>O<sub>3</sub> / (PVA + PEG) Nanocomposite films; synthesis, optical, and dielectric characterizations. *J. Mater. Sci.* **49**, 5378–5387 (2014)
- B.H. Rubee, S. Abd AlHussien, Study of optical properties for (PVA-PEG-ZnO) nanocomposites. *Int. J. Sci. Res. (IJSR)* **5**(5), 1794–1799 (2016)
- K. Borgohain, J.B. Singh, M.R. Rao, T. Shripathi, S. Mahamuni, Quantum size effects in CuO nanoparticles. *Phys. Rev. B* **61**, 11093 (2000)
- F. Marabelli, G.B. Parravicini, F. Salghetti-Drioli, Optical gap of CuO. *Phys. Rev. B* **52**(1433), 1–4 (1995)
- T. Ito, H. Yamaguchi, T. Masumi, S. Adachi, Optical properties of CuO studied by spectroscopic ellipsometry. *J. Phys. Soc. Jpn.* **67**, 3304–3309 (1998)
- F.P. Koffyberg, F.A. Benko, A photoelectrochemical determination of the position of the conduction and valence band edges of p-type CuO. *J. Appl. Phys.* **53**, 1173–1177 (1982)
- J. Ghijsen, L.H. Tjeng, J. van Elp, H. Eskes, J. Westerink, G.A. Sawatzky, M.T. Czyzyk, Electronic structure of Cu<sub>2</sub>O and CuO. *Phys. Rev. B* **38**(11322), 1–9 (1988)
- A.P. Wanninayake, S. Gunashekar, S. Li, B.C. Church, N. Abu-Zahra, Performance enhancement of polymer solar cells using copper oxide nanoparticles. *Semicond. Sci. Technol.* **30**, 064004 (2015)
- A.M. El Sayed, S. El-Gamal, W.M. Morsi, G. Mohammed, Effect of PVA and copper oxide nanoparticles on the structural, optical, and electrical properties of carboxymethyl cellulose films. *J. Mater. Sci.* **50**, 4717–4728 (2015)
- A. Hadi, A. Hashim, Development of a new humidity sensor based on (carboxymethyl cellulose–starch) blend with copper oxide nanoparticles. *Ukr. J. Phys.* **62**(12), 1044–1049 (2017)
- R. Javed, M. Ahmed, I. Ul Haq, S. Nisa, M. Zia, PVP and PEG doped CuO nanoparticles are more biologically active: antibacterial, antioxidant, antidiabetic and cytotoxic perspective. *Mater. Sci. Eng. C* **79**, 108–115 (2017)
- J.K. Rao, A. Raizada, D. Ganguly, M.M. Mankad, S.V. Satyanarayana, G.M. Madhu, Investigation of structural and

- electrical properties of novel CuO–PVA nanocomposite films. *J. Mater. Sci.* **50**, 7064–7074 (2015)
26. J.K. Rao, A. Raizada, D. Ganguly, M.M. Mankad, S.V. Satyanarayana, G.M. Madhu, Enhanced mechanical properties of polyvinyl alcohol composite films containing copper oxide nanoparticles as filler. *Polym. Bull.* **72**, 2033–2047 (2015)
  27. A. Manjunath, M. Irfan, K.P. Anushree, K.M. Vinutha, N. Yamunarani, Synthesis and characterization of CuO nanoparticles and CuO Doped PVA nanocomposites. *Adv. Mater. Phys. Chem.* **10**, 263 (2016)
  28. K. Delgado, R. Quijada, R. Palma, H. Palza, Polypropylene with embedded copper metal or copper oxide nanoparticles as a novel plastic antimicrobial agent. *Lett. Appl. Microbiol.* **53**, 50–54 (2011)
  29. L.N. Shubha, P. Madhusudana Rao, Temperature characterization of dielectric permittivity and AC conductivity of nano copper oxide-doped polyaniline composite. *J. Adv. Dielectr.* **6**(3), 1650018 (2016)
  30. D.M. Jundale, S.T. Navale, G.D. Khuspe, D.S. Dalavi, P.S. Patil, V.B. Patil, Polyaniline–CuO hybrid nanocomposites: synthesis, structural, morphological, optical and electrical transport studies. *J. Mater. Sci.: Mater. Electron.* **24**, 3526–3535 (2013)
  31. M.B. Mohamed, M.H. Abdel-Kader, Effect of excess oxygen content within different nano-oxide additives on the structural and optical properties of PVA/PEG blend. *Appl. Phys.* **125**, 209 (2019)
  32. V. Balan, C.-T. Mihai, F.-D. Cojocaru, C.-M. Uritu, G. Dodi, D. Botezat, I. Gardikiotis, Vibrational spectroscopy fingerprinting in medicine: from molecular to clinical practice. *Materials* **12**(18), 1–40 (2019)
  33. F.H. Falqi, O.A. Bin-Dahman, M. Hussain, M.A. Al-Harhi, Preparation of miscible PVA/PEG blends and effect of graphene concentration on thermal, crystallization, morphological, and mechanical properties of PVA/PEG (10 wt%) blend. *Int. J. Polym. Sci.* (2018). <https://doi.org/10.1155/2018/8527693>
  34. M. Pandey, G.M. Joshi, N.N. Ghosh, Electrical performance of lithium ion based polymer electrolyte with polyethylene glycol and polyvinyl alcohol network. *Int. J. Polym. Mater. Polym. Biomater.* **65**(15), 759–768 (2016)
  35. M. Abdelaziz, Cerium (III) doping effects on optical and thermal properties of PVA films. *Phys. B* **406**(6–7), 1300–1307 (2011)
  36. K. Varatharajan, S. Govindaraj, Structural, optical and dielectric properties of PbS-PVA-PEG nanocomposite film. *Sci. Adv. Mater.* **4**(12), 1247–1253 (2012)
  37. M. Diantoro, T. Istirohah, A. Fuad, I. Ristanti, Dielectric properties and bioactivity of PVA/PEG/TiO<sub>2</sub> fibers for capacitive based body sensor. *J. Phys.* **1040**, 012045 (2018)
  38. E.M. Abdelrazek, I.S. Elashmawi, A. El-khodary, A. Yassin, Structural, optical, thermal and electrical studies on PVA/PVP blends filled with lithium bromide. *Curr. Appl. Phys.* **10**, 607–613 (2010)
  39. R. Singh, S.G. Kulkarni, Thermal and mechanical properties of nano-titanium dioxide-doped polyvinyl alcohol. *Polym. Bull.* **70**, 1251–1264 (2013)
  40. A.M. Shehap, Thermal and spectroscopic studies of polyvinyl alcohol/sodium carboxy methyl cellulose blends. *Egypt. J. Solids* **31**, 75–91 (2008)
  41. J.Q. Almarashi, M.H. Abdel-Kader, Exploring Nano-Sulfide Enhancements on the optical, structural and thermal properties of polymeric nanocomposites. *J. Inorg. Organomet. Polym. Mater.* (2020). <https://doi.org/10.1007/s10904-020-01482-0>
  42. M.B. Mohamed, M.H. Abdel-Kader, SnS<sub>2</sub>/polycarbonate nanocomposites: structural and optical characterization. *J. Inorg. Organomet. Polym. Mater.* (2020). <https://doi.org/10.1007/s10904-019-01364-0>
  43. M.B. Mohamed, M.H. Abdel-Kader, Effect of excess oxygen content within different nano-oxide additives on the structural and optical properties of PVA/PEG blend. *Appl. Phys. A* **125**, 209 (2019)
  44. M.H. Abdel-Kader, M.B. Mohamed, Exploring the direct effect of intermediate band semiconductor materials on the structural, thermal and optical properties of PMMA nanocomposite. *App. Phys. A* **126**, 89 (2020)
  45. M.B. Mohamed, M.H. Abdel-Kader, Effect of annealed ZnS nanoparticles on the structural and optical properties of PVA polymer nanocomposite. *Mater. Chem. Phys.* **241**, 122285 (2020)
  46. A. Hashim, Q. Hadi, Synthesis of novel (polymer blend-ceramics) nanocomposites: structural, optical and electrical properties for humidity sensors. *J. Inorg. Organomet. Polym. Mater.* **28**, 1394–1401 (2018)
  47. K. Ramamohan, V.B. Achari, A.K. Sharma, L. Xiuyang, Electrical and structural characterization of PVA/PEG polymer blend electrolyte films doped with NaClO<sub>4</sub>. *Ionics* **21**(5), 1333–1340 (2015)
  48. G. Attia, M.A. El-Kader, Structural, optical and thermal characterization of PVA/2HEC polyblend films. *Int. J. Electrochem. Sci.* **8**, 5672–5687 (2013)
  49. K.J. Kadhim, I.R. Agool, A. Hashim, Enhancement in optical properties of (PVA-PEG-PVP) blend by the addition of titanium oxide nanoparticles for biological application. *Adv. Environ. Biol.* **10**(1), 81–91 (2016)
  50. N.H. El Fewaty, A.M. El Sayed, R.S. Hafez, Synthesis, structural and optical properties of tin oxide nanoparticles and its CMC/PEG–PVA nanocomposite films. *Composites* **58**(6), 1004–1016 (2016)
  51. D. Beysens, P. Calmettes, Temperature dependence of the refractive indices of liquids: deviation from the Lorentz-Lorenz formula. *J. Chem. Phys.* **66**, 766–771 (1977)
  52. E.A. Costner, B.K. Long, C. Navar, S. Jockusch, X. Lei, P. Zimmerman, A. Campion, N.J. Turro, C. Willson, Fundamental optical properties of linear and cyclic alkanes: VUV absorbance and index of refraction. *J. Phys. Chem. A* **113**, 9337–9347 (2009)
  53. M.Q. Al-Gunaid, T.E. Somesh, H.M. Gayitri, F.H. Al-Ostoot, S. Basavarajaiah, Optimized nano-perovskite lanthanum cuprate decorated PVA based solid polymer electrolyte. *Polym.-Plast. Technol. Mater.* **59**(2), 215–229 (2020)
  54. G. Maroulis, D. Xenides, Dipole, dipole–quadrupole, and dipole–octopole polarizability of adamantane, C<sub>10</sub>H<sub>16</sub>, from refractive index measurements, depolarized collision-induced light scattering, conventional ab initio and density functional theory calculations. *J. Chem. Phys.* **115**(17), 7957–7967 (2001)
  55. D. Sainova, A. Zen, H.-G. Nothofer, U. Asawapirom, U. Scherf, R. Hagen, T. Bieringer, S. Kostromine, D. Neher, Photoaddressable alignment layers for fluorescent polymers in polarized electroluminescence devices. *Adv. Funct. Mater.* **12**(1), 49–57 (2002)
  56. M. Caglar, M. Zor, S. Ilican, Y. Caglar, Effect of indium incorporation on the optical properties of spray pyrolyzed Cd<sub>0.22</sub>Zn<sub>0.78</sub>S thin films. *Czech J. Phys.* **56**, 277–287 (2006)
  57. O.G. Abdullah, S.B. Aziz, K.M. Omer, Y.M. Salih, Reducing the optical band gap of polyvinyl alcohol (PVA) based nanocomposite. *J. Mater. Sci* **26**, 5303–5309 (2015)
  58. A.M. Shehap, D.S. Akil, Structural and optical properties of TiO<sub>2</sub> nanoparticles/PVA for different composites thin films. *Int. J. Nanoelectron. Mater.* **9**, 17–36 (2016)
  59. A.A. Alhazime, M.B. Mohamed, M.H. Abdel-Kader, Effect of Zn<sub>1-x</sub>Mg<sub>x</sub>S doping on structural, thermal and optical properties of PVA. *J. Inorg. Organomet. Polym. Mater.* **29**(2), 436–443 (2019)
  60. F.F. Muhammad, S.B. Aziz, S.A. Hussein, Effect of the dopant salt on the optical parameters of PVA:NaNO<sub>3</sub> solid polymer electrolyte. *J. Mater. Sci.: Mater. Electron.* **26**, 521–529 (2015)
  61. S.B. Aziz, H.M. Ahmed, A.M. Hussein, A.B. Fathulla, R.M. Wsw, R.T. Hussein, Tuning the absorption of ultraviolet spectra and



- optical parameters of aluminum doped PVA based solid polymer composites. *J. Mater. Sci.: Mater. Electron.* **26**, 8022–8028 (2015)
62. M.B. Mohamed, M.H. Abdel-Kader, A.A. Alhazime, J.Q. Almarashi, Effect of preparation methods and doping on the structural and tunable emissions of Cd. *J. Mol. Struct.* **1155**, 666–674 (2018)
63. L.Y. Jua, R.R. Karri, N.M. Mubarak, L.S. Yon, C.H. Bing, M. Khalid, P. Jagadish, E.C. Abdullah, Modeling of methylene blue adsorption using functionalized buckypaper/polyvinyl alcohol membrane via ant colony optimization. *Environ. Pollut.* **259**, 113940 (2020)
64. M.B. Mohamed, M.H. Abdel-Kader, A.A. Alhazime, Structural and optical properties of doped ZnO/SiO<sub>2</sub> nanocomposite. *Int. J. Appl. Ceram. Technol.* **16**(3), 1209–1217 (2019)
65. M.B. Mohamed, M.H. Abdel-Kader, J.Q. Almarashi, Role of Cu/S ratio and Mg doping on modification of structural and optical characteristics of nano CuS. *Int. J. Appl. Ceram. Technol.* **17**(2), 832–840 (2020)

**Publisher's Note** Springer Nature remains neutral with regard to jurisdictional claims in published maps and institutional affiliations.